

Compositional design and microstructure analysis of Zr-based bulk metallic glasses

YAN Ming(严明)^{1,2}, ZOU Jin(邹进)², SHEN Jun(沈军)¹, SUN Jian-fei(孙剑飞)¹

1. School of Materials Science and Engineering, Harbin Institute of Technology, Harbin 150001, China;
2. School of Engineering and Centre for Microscopy and Microanalysis, University of Queensland, QLD 4072, Australia

Received 15 July 2007; accepted 10 September 2007

Abstract: The systematical studies of Zr-based BMGs were summarized in terms of their compositional design and their structural characterization. In particular, several key issues of BMG materials were focused, including initial alloy design and subsequent composition optimization, solidification microstructure characterization and crystallization process specification. The results show that a compositional designing approach is successfully developed and, through extensive microstructure characterization using transmission electron microscopy, several new crystalline phases are discovered in these newly developed Zr-based BMG alloys. Crystallization behavior of Zr-based BMG is also determined based on the microstructure analysis.

Key words: metallic glass; microstructure characterization; solidification; crystallization

1 Introduction

Metallic glass was firstly developed in the 1960s[1]. Extremely high cooling rate (about 10^6 K/s) was required to avoid crystallization during the melt cooling process, which could only be achieved through highly specific equipments and, in general, the dimensions of resultant glasses were less than tens of micrometers. These disadvantages have restricted the study of metallic glasses till the discoveries of Pd-based[2] and Ln-based [3] metallic glasses in the 1980s, whose critical dimensions are in the scale of millimeter and consequently open the door for the research of so-called bulk metallic glasses(BMGs) that have a much higher glass forming ability and can be fabricated via conventional casting facilities. Since then, numerous BMG systems have been developed due to their superior properties over the crystalline counterparts, which make them a promising candidate as structural and functional materials for many engineering applications. Among them, Zr-based BMGs have shown several outstanding characters[4–7]: high glass forming ability;

high thermal stability; superior mechanical properties, including high strength at room temperature and super-plasticity at room and high temperatures. These advantages make Zr-based BMGs one of the most favorite BMG systems scientifically and technologically.

Although enormous progresses have been achieved so far in the development of BMGs, there are still several fundamentals that deserve further investigations, such as alloy designing, solidification and crystallization analysis. In this work, some fundamental issues were summarized, including alloy designing and microstructure characterization in the Zr-based BMGs.

2 Compositional design

How to design alloys that favor the glass formation rather than crystallization is probably the most important issue in the BMG field. On this point, several well-known experimental principles, such as “Three Empirical Principles”[8] and “Confusion by Design”[9] have been well accepted and applied in the BMG field. However, these approaches still require a large amount of tedious experiments. Following these routes, extensive

searching and screening processes for glass forming alloys are still unavoidable.

In order to determine the BMG compositions more efficiently, based on the study of binary phase diagrams associated with compositions in the Zr-based BMG systems, we have developed a composition design approach that can predict high glass forming ability of BMG forming alloys with very limited experiments. The principle of this approach[10] can be summarized as follows. It is well documented that the glass formation requires suppression of the nucleation and growth of the competing crystalline phases. If the chemical affinity between the atomic pairs of the constitutional elements can be balanced in a certain degree (instead of forming crystals), the designed alloys would have a strong ability to prevent the precipitation of any crystalline compounds from the melt during the cooling process. In this newly developed approach, we have demonstrated that such a balance in the chemical affinity can be achieved by proportionally mixing the corresponding binary eutectic compositions with low eutectic points.

By applying this newly developed approach to the Zr-based alloys, we have successfully developed several Zr-based BMGs with high glass forming abilities[10–13]. Table 1 lists a few representative alloys. Among them, $Zr_{51}Cu_{20.7}Ni_{12}Al_{16.3}$ shows an extremely high T_g (the glass transition temperature) value and significant mechanical properties. Furthermore, the composition-tuned alloys $(Zr_{0.593}Cu_{0.187}Ni_{0.12}Al_{0.10})_{96}Ti_4$ and $(Zr_{0.51}Cu_{0.207}Ni_{0.12}Al_{0.163})_{99.5}Y_{0.5}$ can be easily cast into rod-shaped amorphous samples with a diameter up to 10 mm via conventional casting facilities, which make them ones of the best glass forming alloys in Zr-based BMGs.

This compositional design approach has also been applied to other BMG systems, such as Cu-[14] and Ni-based[15] BMGs. The significance of this approach lies in its efficiency and easiness to locate a specific composition that favors the glass formation in a given system. Based on the designed alloy, the subsequent composition optimization by appropriately adjusting the contents of the constitutional elements or by adding

alloying elements can further improve the glass forming ability. Some examples are shown in Table 1, i.e., $Zr_{51}Cu_{20.7}Ni_{12}Al_{16.3} \rightarrow (Zr_{0.51}Cu_{0.207}Ni_{0.12}Al_{0.163})_{99.5}Y_{0.5}$ and $Zr_{59.3}Cu_{18.7}Ni_{12}Al_{10} \rightarrow (Zr_{0.593}Cu_{0.187}Ni_{0.12}Al_{0.10})_{96}Ti_4$, or in Ref.[16].

3 Solidification microstructure characterization

Since materials property depends strongly upon their microstructures, it is essential to determine materials microstructures so as to fundamentally understand their properties. In the case of BMGs, it is critically necessary to evaluate the solidification microstructures to justify the amorphous state as well as to specify the resultant products of the solidification process. If in-situ crystallization takes place, even at very earlier stage, identifying the crystalline phase(s) is critically important to avoid them in the future alloy design. In a recent study, HUFNAGEL[17] stressed the importance of the study of fine microstructure in amorphous materials. Our previous studies[5,13] have shown that the investigation of quenched-in crystalline phases can provide insights on which phases are the competing phases to the amorphous structure, which is vital to understand the impurity effects.

Table 2 lists crystalline phases found in Zr-based BMGs[18–36]. It should be noted that some of these phases were reported as the quench-in phases while the others were observed in the annealing process. However, an attempt to clearly differentiate them remains impossible, because, in fact, these phases could be formed in both processes. From Table 2, one can also realize the complexity of identification of these crystalline phases. This complexity mainly results from two aspects: 1) most of Zr-based BMGs contain more than three components and their relative compositions vary; 2) the quenching process and/or the annealing process can vary significantly, too.

Traditionally, the X-ray diffraction (XRD) technique has been the primary technique to determine

Table 1 Thermal data for representative Zr-based BMGs developed in our group with well-known alloy $Zr_{65}Cu_{17.5}Ni_{10}Al_{7.5}$ for simple comparison

Zr-based BMGs	T_g/K	T_x/K	$\Delta T_x/K$	T_l/K	T_{rg}	D/mm	Ref.
$Zr_{59.3}Cu_{18.7}Ni_{12}Al_{10}$	670	772	102	1 080	0.620	~3	[11]
$(Zr_{0.593}Cu_{0.187}Ni_{0.12}Al_{0.10})_{96}Ti_4$	669	747	78	1 029	0.650	~10	[12]
$Zr_{51}Cu_{20.7}Ni_{12}Al_{16.3}$	722	800	78	1 132	0.638	~3	[13]
$(Zr_{0.51}Cu_{0.207}Ni_{0.12}Al_{0.163})_{99.5}Y_{0.5}$	725	802	77	1 130	0.642	~10	[13]
$Zr_{65}Cu_{17.5}Ni_{10}Al_{7.5}$	657	736	99	1 168	0.562	~5	[13]

T_l : Liquidus temperature; D : Largest achievable diameter with amorphous structure

Table 2 Crystalline phases reported in some Zr-based BMG forming alloys

Phase	Zr-based BMG	Crystal structure and unit cell parameters (in nm)	Ref.
Al _{1.7} Ni _{0.3} Zr	Zr _{52.5} Cu ₂₇ Ni ₈ Al ₁₀ Ti _{2.5}	C, Fd3m: $a=0.738$	[18]
AlZr	Zr ₆₅ Al _{7.5} Ni ₁₀ Cu _{12.5} Ag ₅	NM, PDF: O, Cmc: $a=0.335$ 9, $b=1.088$, $c=0.427$	[19]
Al ₂ Zr	(Cu _{0.50} Zr _{0.50}) ₉₈ Al ₂	NM, PDF: H, P6 ₃ /mmc: $a=0.528$, $c=0.874$; O: $a=0.104$, $b=0.721$, $c=0.497$	[20]
Al ₃ Zr ₄	Zr _{52.5} Ni _{14.6} Al ₁₀ Cu _{17.9} Ti ₅	NM, PDF: H, P($\bar{6}$): $a=0.543$, $c=0.539$	[21]
Cu(Al, Ni)Zr ₂	Zr ₆₅ Al _{7.5} Ni ₁₀ Cu ₂₀	T, I4/MMM: $a=0.323$ 8, $c=1.111$	[22]
Cu ₁₀ Zr ₇	Zr ₅₅ Al ₁₅ Ni ₁₀ Cu ₂₀	NM, PDF: O, C2ca: $a=1.267$, $b=0.931$, $c=0.935$	[23]
Cu ₅₁ Zr ₁₄	(Cu _{0.50} Zr _{0.50}) ₉₈ Al ₂	H, P6/m: $a=1.123$, $c=0.827$	[20]
NiZr	Zr ₆₅ Al _{7.5} Ni ₁₀ Cu _{12.5} Ag ₅	NM, PDF: O, Cmc: $a=0.326$, $b=0.997$, $c=0.408$; X-type phase	[19]
NiZr ₂	Zr ₅₇ Ti ₈ Nb _{2.5} Cu _{13.9} Ni _{11.1} Al _{7.5}	T, I4/mcm: $a=0.651$, $c=0.524$	[24]
Ni ₁₀ Zr ₇	Zr _{52.5} Ni _{14.6} Al ₁₀ Cu _{17.9} Ti ₅	O, Ab2a: $a=0.922$, $b=1.229$, $c=0.915$	[21]
Zr(Ag, Ni)	Zr ₆₅ Al _{7.5} Ni ₁₀ Cu _{12.5} Ag ₅	NM, no data in PDF database	[19]
ZrAl	Zr _{52.5} Ni _{14.6} Al ₁₀ Cu _{17.9} Ti ₅	O, Cmc: $a=0.335$ 9, $b=1.088$, $c=0.427$ 4	[25]
Zr ₂ Al	Zr ₆₀ Al ₁₀ Cu _{30-x} Pd _x ($x=0, 10$)	NM, PDF: H, P6 ₃ /mmc: $a=0.489$, $c=0.593$; T, I4/mcm: $a=0.685$, $c=0.550$	[26]
Zr ₃ Al	Zr _{52.25} Cu _{28.5} Ni _{4.75} Al _{9.5} Ta ₅	C, Pm3m: $a=0.437$ 2	[27]
Zr ₃ Al ₂	Zr ₆₀ Al ₁₀ Cu _{30-x} Pd _x ($x=0, 10$)	T, P4 ₂ /mmn: $a=0.762$, $c=0.699$	[26]
ZrAlCu ₂	Zr ₅₅ Cu ₃₀ Al ₁₀ Ni ₅	C, Fm3m: $a=0.621$ 5	[28]
Zr ₆ AlNi ₂	Zr ₆₅ Al _{7.5} Ni ₁₀ Cu ₂₀	H, p6($\bar{2}$)m: $a=0.792$, $c=0.334$	[22]
Zr(Al, Ni) ₂	Zr _{52.5} Ni _{14.6} Al ₁₀ Cu _{17.9} Ti ₅	C, Fd3m: $a=0.612$ 3	[21]
Zr ₂ Cu	Zr ₆₅ Al _{7.5} Ni ₁₀ Cu ₂₀	T, I4/mmm: $a=0.453$ 6, $c=0.371$ 6	[29]
Zr ₂ (Cu, Al)	Zr ₆₅ Al _{7.5} Cu _{27.5}	NM, C typed crystal, no data in PDF database	[30]
Zr ₂ (Cu, Al)	Zr ₆₅ Al _x Cu ₃₅	NM, T typed crystal, no data in PDF database	[31]
Zr ₇ Cu ₄ Al ₃ O	Zr ₅₅ Al ₁₅ Ni ₁₀ Cu ₂₀	C, Fd($\bar{3}$)m: $a=0.57$	[32]
Zr ₇₂ Cu ₁₆ Al ₈ O ₄	Zr ₆₅ Cu _{27.5} Al _{17.5}	Quasicrystal	[30]
Zr _{35.4} Cu _{24.0} Ni _{9.3} Al _{31.3}		R: $a=0.540$, $c=2.910$	[33]
Zr _{47.6} Cu _{22.4} Ni _{14.2} Al _{15.8}	(Zr _{0.51} Cu _{0.207} Ni _{0.12} Al _{0.163}) _{100-x} Y _x ($x=0.75$ and 1)	O: $a=0.69$, $b=0.75$, $c=0.74$	[5]
Zr _{57.1} Cu _{24.0} Ni _{8.1} Al _{10.8}		M: $a=0.951$, $b=0.546$, $c=1.015$, $\beta=72^\circ$	[33]
Zr ₄ Cu ₂ O	Zr ₅₅ Cu ₃₀ Al ₁₀ Ni ₅	C, Fd($\bar{3}$)m: $a=1.227$	[34]
Zr ₂ Ni	Zr _{69.5} Cu ₁₂ Ni ₁₁ Al _{7.5}	T, I4/mcm: $a=0.648$ 6, $c=0.527$ 9	[24]
	Zr ₅₅ Al ₁₅ Ni ₁₀ Cu ₂₀	C, Fd3m: $a=1.227$	[22]
Zr ₂ (Ni _{0.67} O _{0.33})	(Hf _x Zr _{1-x}) _{52.5} Cu _{17.9} Ni _{14.6} Al ₁₀ Ti ₅	T-type phase	[25]
Zr ₄ Ni ₂ O	Zr _{52.5} Ni _{14.6} Al ₁₀ Cu _{17.9} Ti ₅	C, Fd($\bar{3}$)m: $a=1.219$ 7	[35]
ZrO ₂	Zr ₆₅ Cu _{27.5} Al _{17.5}	NM, PDF: M, P2 ₁ /c: $a=0.515$, $b=0.521$, $c=0.532$, $\beta=99.216^\circ$; O, Pnam: $a=0.547$, $b=0.634$, $c=0.325$; T, P4 ₂ /nmc: $a=0.360$, $c=0.518$	[36]

NM, PDF: Crystal structure not given in Ref. and data suggested by PDF database; C: Cubic; T: Tetragonal; H: Hexagonal; O: Orthorhombic; R: Rhombohedral; M: Monoclinic; X: Unspecified structure

the crystalline phases. However, there are two fundamental limitations that have fatally restricted the power of XRD in specifying the crystalline phases in the field of BMGs: 1) XRD requires a considerable amount of a crystalline phase to show up its diffraction peaks. If the content of a crystalline phase is small (which is particularly true for a partially crystallized

microstructure), XRD fails. 2) In general, several crystalline phases co-exist in a BMG system, this situation, in some cases, makes XRD an unreliable technique to identify crystalline phases. This situation can often be coupled with the fact that the crystalline phases found in the BMGs are often not the pure phases listed in the Joint Committee on Powder Diffraction

Standards. This leads to the deviation of standard and measured lattice parameter(s) for a given phase, which enhances the complication in analyzing the XRD data. To avoid these problems, we have successfully employed transmission electron microscopy (TEM) to investigate the crystalline phases in BMGs as TEM is a powerful tool to study local structure in the real (image) and reciprocal (diffraction) spaces. Through applying TEM, new crystalline phases [5,33] and the competing phases to the amorphous structure [37–38] have been identified.

Fig.1 shows the bright-field TEM images and corresponding selected area electron diffraction (SAED) patterns for two recently discovered crystalline phases in a slowly cooled $Zr_{51}Cu_{20.7}Ni_{12}Al_{16.3}$ alloy. Based on the diffraction information, they were determined as a rhombohedral structured crystal with lattice parameters (in hexagonal unit cell) of $a=0.540$ nm and $c=2.910$ nm, and a monoclinic structured crystal with lattice parameters of $a=0.951$ nm, $b=0.546$ nm, $c=1.015$ nm and $\beta=72^\circ$. The energy dispersive spectroscopy facility attached in the TEM confirmed their averaged

compositions as $Zr_{35.4}Cu_{24.0}Ni_{9.3}Al_{31.3}$ and $Zr_{57.1}Cu_{24.0}Ni_{8.1}Al_{10.8}$, respectively. In addition, an orthorhombic phase, with lattice parameters of $a=0.69$ nm, $b=0.75$ nm and $c=0.74$ nm, was also determined in the yttrium doped $Zr_{51}Cu_{20.7}Ni_{12}Al_{16.3}$ alloys [5]. From these examples, we anticipate that there should be many new phases existing in the BMGs, and TEM should be the unique tool in their identifications.

As an example of competing phase to the amorphous structure, an oxygen stabilized face centered cubic $NiZr_2$ ($a=1.22$ nm) was observed in 5 mm $Zr_{51}Cu_{20.7}Ni_{12}Al_{16.3}$ alloy as the single phase surrounded by the amorphous matrix. Figs.2(a) and (b) show its bright-field TEM image and corresponding SAED patterns. Based on this, yttrium was introduced as an oxygen getter element. TEM analysis confirmed that the formation of the body centered cubic Y_2O_3 ($a=1.05$ nm) phase, as evidenced in Figs.2(c) and (d). TEM images show that, apart from these Y_2O_3 crystalline particles, the remaining is amorphous, confirming that adding yttrium is a very effective route in enhancing the glass

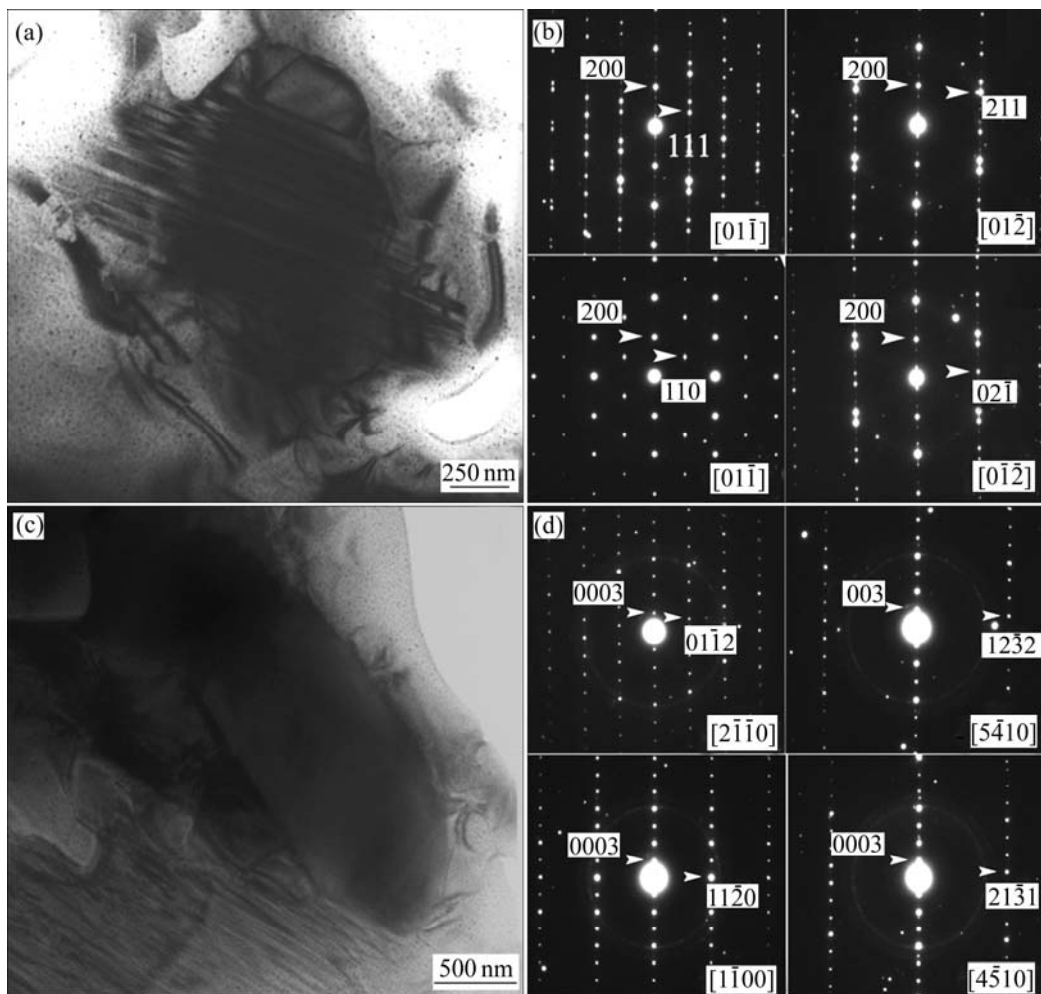


Fig.1 TEM bright-field images and corresponding SAED patterns for two new phases observed in slowly cooled $Zr_{51}Cu_{20.7}Ni_{12}Al_{16.3}$ alloy: (a), (b) Rhombohedral phase; (c), (d) Monoclinic phase

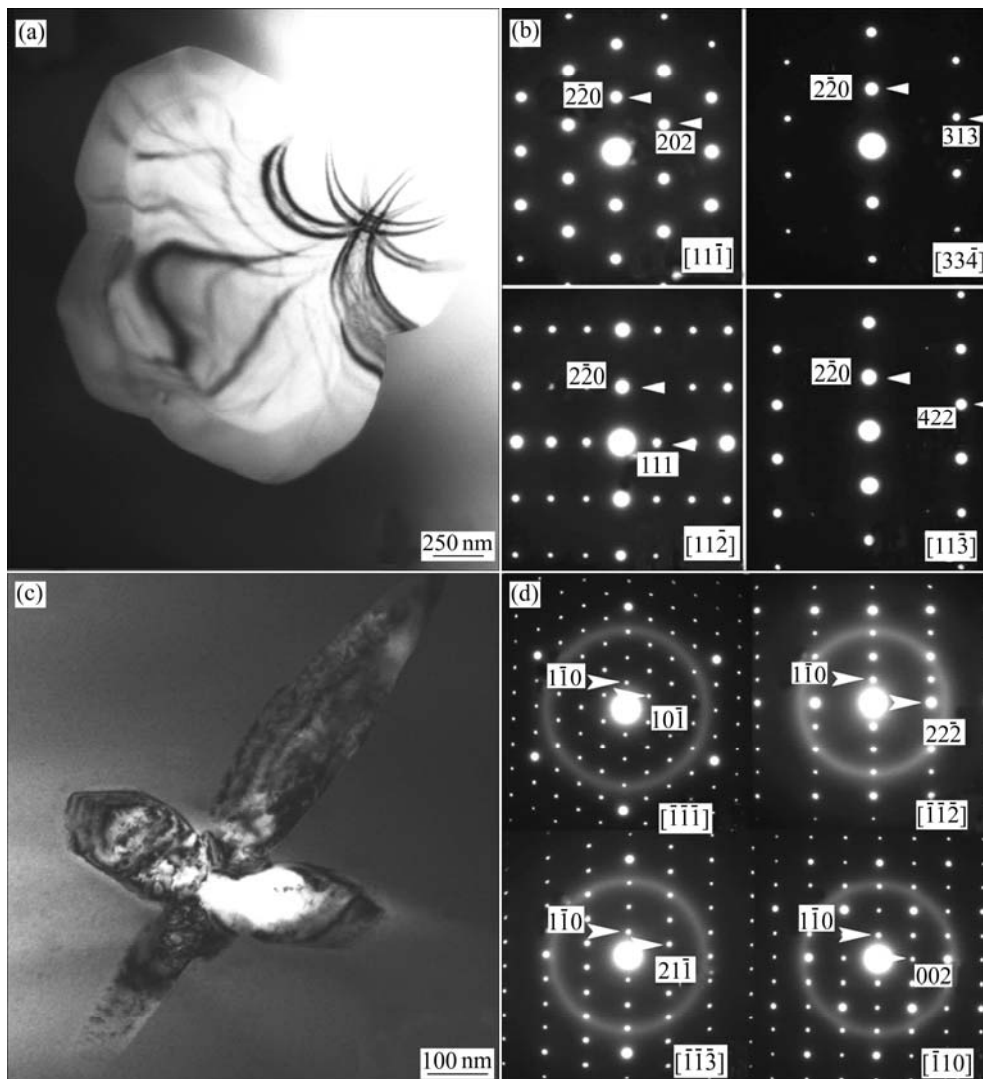


Fig.2 TEM bright-field image (a) showing competing phase (NiZr_2 type) in $d5 \text{ mm}$ $\text{Zr}_{51}\text{Cu}_{20.7}\text{Ni}_{12}\text{Al}_{16.3}$ alloy with series of SAED patterns (b), and TEM bright-field image (c) showing body centered cubic Y_2O_3 phase found in yttrium-doped $\text{Zr}_{51}\text{Cu}_{20.7}\text{Ni}_{12}\text{Al}_{16.3}$ alloy with series of SAED patterns (d)

glass forming ability.

4 Thermal stability and crystallization behavior analysis

Since BMGs are in a thermodynamically metastable state compared with their crystalline counterparts, evaluating their thermal stability is necessary from a viewpoint of their industrial applications. Conventionally, there are several characteristic parameters can be used to assess the thermal stability[8], they are: T_g , T_x (the crystallization temperature) and $\Delta T_x (= T_x - T_g)$, and the calculated activation energies at certain temperatures, such as E_g (the activation energy at the glass transition temperature), and E_p (the activation energy at the peak temperature of crystallization). While controversies are often encountered when using different parameters due to the inconsistency between them, more reliable and

more direct methods should be used to solve these problems.

Fig.3 shows the high resolution TEM images and SAED patterns for the as-prepared and annealed alloys $\text{Zr}_{51}\text{Cu}_{20.7}\text{Ni}_{12}\text{Al}_{16.3}$ and $\text{Zr}_{65}\text{Cu}_{17.5}\text{Ni}_{10}\text{Al}_{7.5}$, respectively [10]. Based on these TEM results, it can be clearly understood that $\text{Zr}_{51}\text{Cu}_{20.7}\text{Ni}_{12}\text{Al}_{16.3}$ has better thermal stability than $\text{Zr}_{65}\text{Cu}_{17.5}\text{Ni}_{10}\text{Al}_{7.5}$ under the identical annealing conditions. However, if just judging from the thermal data shown in Table 1, one cannot distinguish which alloy is more thermally stable, since the former alloy has higher T_g value, yet the latter one has a higher ΔT_x value.

The crystallization behavior study is another important issue for BMGs. It is well known that the devitrification and the crystallization of BMGs are fundamental pathways to generate nano-crystals[39]. At the same time, some partially crystallized BMGs show

the increase of strength, and even ductility, when compared with their fully amorphous counterparts, which has attracted great attentions both scientifically and technologically[8].

By using electron microscopy techniques, one can obtain the information on the following aspects of the

crystallization behavior: the primary phases (including the structures and compositions), the nucleation and growth processes, and the crystallization products. Fig.4 shows the TEM results of the annealed alloy $(\text{Zr}_{0.51}\text{Cu}_{0.207}\text{Ni}_{0.12}\text{Al}_{0.163})_{99.5}\text{Y}_{0.5}$, which shows a tetragonal structured phase with large lattice parameters

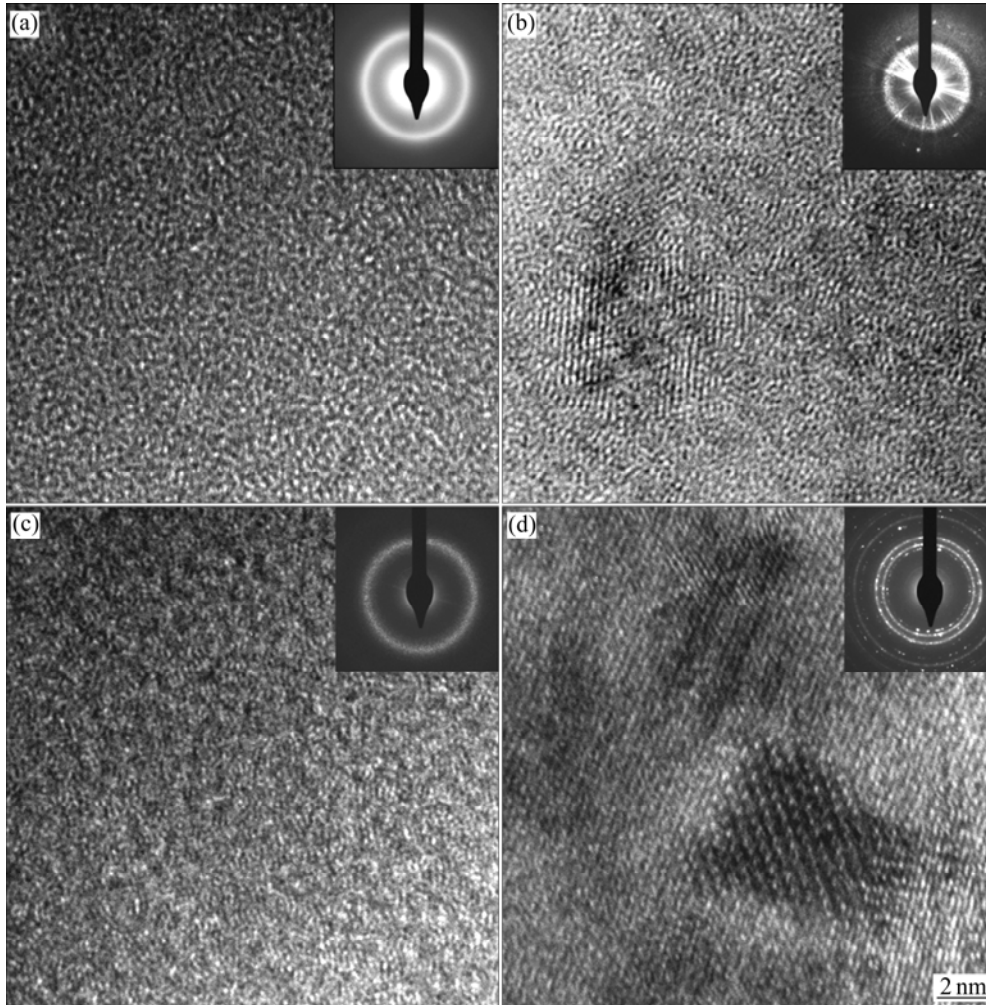


Fig.3 High-resolution TEM images and corresponding SAED patterns (insets) for as-prepared $\text{Zr}_{51}\text{Cu}_{20.7}\text{Ni}_{12}\text{Al}_{16.3}$ alloy (a), as-prepared $\text{Zr}_{65}\text{Cu}_{17.5}\text{Ni}_{10}\text{Al}_{7.5}$ alloy (b), $\text{Zr}_{51}\text{Cu}_{20.7}\text{Ni}_{12}\text{Al}_{16.3}$ alloy annealed at 673 K for 60 min (c) and $\text{Zr}_{65}\text{Cu}_{17.5}\text{Ni}_{10}\text{Al}_{7.5}$ alloy annealed at 673 K for 60min (d)

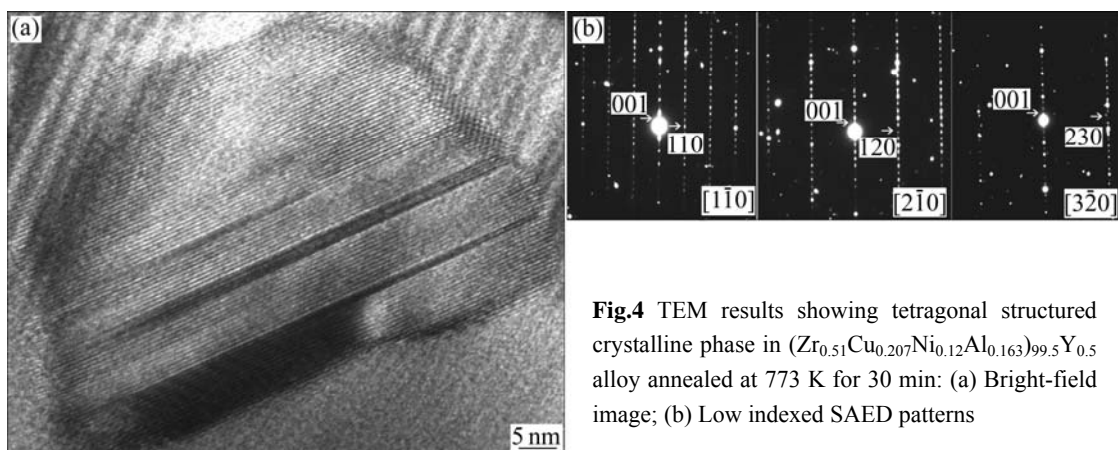


Fig.4 TEM results showing tetragonal structured crystalline phase in $(\text{Zr}_{0.51}\text{Cu}_{0.207}\text{Ni}_{0.12}\text{Al}_{0.163})_{99.5}\text{Y}_{0.5}$ alloy annealed at 773 K for 30 min: (a) Bright-field image; (b) Low indexed SAED patterns

($a=0.96$ nm and $c=2.82$ nm)[40]. Since this phase disappears in the subsequent high temperature treatments, suggesting that this phase is a metastable phase that will transfer into other stable phases.

5 Conclusions

1) A BMG design approach has been developed and has successfully predicted alloy compositions that favor the glass forming process. The advantage of this approach lies in its easiness of locating multi-component alloy compositions. The efficiency of this approach has been demonstrated in Zr-based BMGs as well as in other glass forming systems.

2) By characterization of the solidification microstructure using TEM, we determined three new crystalline phases in the slowly cooled alloy $Zr_{51}Cu_{20.7}Ni_{12}Al_{16.3}$ and $(Zr_{0.51}Cu_{0.207}Ni_{0.12}Al_{0.163})_{100-x}Y_x$ ($x=0.75$ and 1), respectively. Based on the TEM analysis of the competing phases to the vitrification, pathways for optimizing the designed alloys have been suggested and a greatly enhanced glass forming ability has been achieved.

3) By characterization of the annealed BMG alloys using TEM, we systematically studied the crystallization behavior of a high GFA alloy, $(Zr_{0.51}Cu_{0.207}Ni_{0.12}Al_{0.163})_{99.5}Y_{0.5}$, and specified its crystallization process and crystallization products. Based on TEM results, we has also verified that the alloy $Zr_{51}Cu_{20.7}Ni_{12}Al_{16.3}$ has a higher thermal stability compared with a well-known alloy $Zr_{65}Cu_{17.5}Ni_{10}Al_{7.5}$, from which the power of TEM is well demonstrated.

References

- [1] CLEMENT W, WILLENS R H, DUWEZ P. Non-crystalline structure in solidified gold-silicon alloys [J]. *Nature*, 1960, 187: 869–870.
- [2] KUI W H, GREER A L, TURNBULL D. Formation of bulk metallic-glass by fluxing [J]. *Appl Phys Lett*, 1984, 45: 615–616.
- [3] INOUE A, ZHANG T, MASUMOTO T. Al-La-Ni amorphous-alloys with a wide supercooled liquid region [J]. *Mater Trans JIM*, 1989, 30: 965–972.
- [4] PEKER A, JOHNSON W L. A highly processable metallic glass: $Zr_{41.2}Ti_{13.8}Cu_{12.5}Ni_{10.0}Be_{22.5}$ [J]. *Appl Phys Lett*, 1993, 63: 2342–2344.
- [5] YAN M, ZOU J, SHEN J. Effect of over-doped yttrium on the microstructure, mechanical properties and thermal properties of a Zr-based metallic glass [J]. *Acta Mater*, 2006, 54: 3627–3635.
- [6] LIU Y H, WANG G, WANG R J, ZHAO D Q, PAN M X, WANG W H. Super plastic bulk metallic glasses at room temperature [J]. *Science*, 2007, 315: 1385–1388.
- [7] WANG G, SHEN J, SUN J F, HUANG Y J, ZOU J, LU Z P, STACHURSKI Z H, ZHOU B D. Superplasticity and superplastic forming ability of a Zr-Ti-Ni-Cu-Be bulk metallic glass in the supercooled liquid region [J]. *J Non-Cryst Solids*, 2005, 351: 209–217.
- [8] INOUE A. Stabilization of metallic supercooled liquid and bulk amorphous alloys [J]. *Acta Mater*, 2000, 48: 279–306.
- [9] GREER A L. Confusion by design [J]. *Nature*, 1993, 366: 303–304.
- [10] SHEN J, ZOU J, YE L, LU Z P, XING D W, YAN M, SUN J F. Glass-forming ability and thermal stability of a new bulk metallic glass in the quaternary Zr-Cu-Ni-Al system [J]. *J Non-Cryst Solids*, 2005, 351: 2519–2523.
- [11] XING Da-wei. Formation and crystallization kinetics of bulk ZrCuNiAlTi metallic glass [D]. Harbin: Harbin Institute of Technology, 2003. (in Chinese)
- [12] XING D W, SUN J F, LI Y Q, WANG G, YAN M, SHEN J. Effect of Ti addition on supercooled liquid region and glass forming ability of bulk amorphous $Zr_{60}Cu_{20}Ni_{10-x}Al_{10}Ti_x$ alloys [J]. *Trans Nonferrous Met Soc China*, 2003, 13(S1): 68–70.
- [13] YAN M, SHEN J, ZHANG T, ZOU J. Enhanced glass-forming ability of a Zr-based bulk metallic glass with yttrium doping [J]. *J Non-Cryst Solids*, 2006, 352: 3109–3112.
- [14] YANG Ying-jun, SUN Jian-fei, LI Yong-ze, SUN Ji-ku, SHEN Jun. Fabrication of Cu-based bulk metallic glasses by binary deep eutectic method [J]. *The Chinese Journal of Nonferrous Metals*, 2005, 15: 1179–1183. (in Chinese)
- [15] LIANG W Z, SHEN J, SUN J F. Effect of Si addition on the glass-forming ability of a NiTiZrAlCu alloy [J]. *J Alloys Compd*, 2006, 420: 94–97.
- [16] SHEN J, CHEN Q J, SUN J F, FAN H B, WANG G. Exceptionally high glass-forming ability of an FeCoCrMoCu alloy [J]. *Appl Phys Lett*, 2005, 86: 151907.1–151907.3.
- [17] HUFNAGEL T C. Amorphous materials-finding order in disorder [J]. *Nat Mater*, 2004, 3: 666–667.
- [18] FATAY D, GUBICZA J, SZOMMER P, LENDVAI J, BLETRY M, GUYOT P. Thermal stability and mechanical properties of a Zr-based bulk amorphous alloy [J]. *Mater Sci Eng A*, 2004, 387/389: 1001–1004.
- [19] KIM S J, HAN T K, KIM Y H, YANG Y S. Crystallization and the formation of nanocrystals in amorphous Zr-Al-Ni-Cu-Ag alloy [J]. *Scripta Mater*, 2001, 44: 1281–1285.
- [20] YU P, BAI H Y, TANG M B, WANG W L. Excellent glass-forming ability in simple Cu₅₀Zr₅₀-based alloys [J]. *J. Non-Cryst Solids*, 2005, 351: 1328–1332.
- [21] WANG J G, CHOI B W, NIEH T G, LIU C T. Crystallization and nanoindentation behavior of a bulk Zr-Al-Ti-Cu-Ni amorphous alloy [J]. *J Mater Res*, 2000, 15: 798–807.
- [22] ECKERT J, MATTERN N, ZINKEVITCH M, SEIDEL M. Crystallization behavior and phase formation in Zr-Al-Cu-Ni metallic glass containing oxygen [J]. *Mater Trans JIM*, 1998, 39: 623–634.
- [23] ZHANG J, WEI Y H, QIU K Q, ZHANG Z F, QUAN M X, HU Z Q. Crystallization kinetics and pressure effect on crystallization of $Zr_{55}Al_{10}Ni_5Cu_{30}$ bulk metallic glass [J]. *Mater Sci Eng A*, 2003, 357: 386–391.
- [24] SCUDINO S, KUHN U, SCHULTZ L, NAGAHAMA D, HONO K, ECKERT J. Microstructure evolution upon devitrification and crystallization kinetics of $Zr_{57}Ti_8Nb_{2.5}Cu_{13.9}Ni_{11.4}Al_{7.5}$ melt-spun glassy ribbon [J]. *J Appl Phys*, 2004, 95: 3397–3403.
- [25] HE G, ZHANG Z F, LOSER W, ECKERT J, SCHULTZ L. Effect of Ta on glass formation, thermal stability and mechanical properties of a $Zr_{52.25}Cu_{28.5}Ni_{4.75}Al_{9.5}Ta_5$ bulk metallic glass [J]. *Acta Mater*, 2003, 51: 2383–2395.
- [26] INOUE A, FAN G. High-strength bulk nanocrystalline alloys containing compound and amorphous phases [J]. *Nanostruct Mater*, 1999, 12: 741–749.
- [27] HE G, BIAN Z, CHEN G L. Investigation of phases on a Zr-based bulk glass alloy [J]. *Mater Sci Eng A*, 2000, 279: 237–243.
- [28] KAI W, HSIEH H H, NIEH T G, KAWAMURA Y. Oxidation behavior of a Zr-Cu-Al-Ni amorphous alloy in air at 300–425

- degrees C [J]. *Intermetallics*, 2002, 10: 1265–1270.
- [29] WANG W H, BIAN Z, WEN P, ZHANG Y, PAN M X, ZHAO D Q. Role of addition in formation and properties of Zr-based bulk metallic glasses [J]. *Intermetallics*, 2002, 10: 1249–1257.
- [30] MURTY B S, PING D H, HONO K, INOUE A. Direct evidence for oxygen stabilization of icosahedral phase during crystallization of $Zr_{65}Cu_{27.5}Al_{7.5}$ metallic glass [J]. *Appl Phys Lett*, 2000, 76: 55–57.
- [31] INOUE A, KAWASE D, TSAI A P, ZHANG T, MASUMOTO T. Stability and Transformation to crystalline phases of amorphous Zr-Al-Cu alloys with significant supercooled liquid region [J]. *Mater Sci Eng A*, 1994, 78: 255–263.
- [32] LEE K S, HA T K, AHN S, CHANG Y W. High temperature deformation behavior of the $Zr_{41.2}Ti_{13.8}Cu_{12.5}Ni_{10}Be_{22.5}$ bulk metallic glass [J]. *J Non-Cryst Solids*, 2003, 317: 193–199.
- [33] YAN M, ZOU J, SHEN J. New crystalline phases formed in a slowly-cooled Zr-based metallic glass [J]. *J Alloys Compd*, 2006, 433: 120–124.
- [34] DE OLIVERIA M F, KAUFMAN M J, BOTTA W J, KIMINAMI C S. The “big-cube” phase found in Zr-Cu-Al-Ni easy glass forming alloys [J]. *Mater Sci Forum*, 2002, 403: 101–106.
- [35] MACKAY R, MILLER G J, FRANZEN H F. New oxides of the filled-Ti₂Ni type-structure [J]. *J Alloys Compd*, 1994, 204: 109–118.
- [36] TRIWIKANTORO, TOMA D, MEURIS M, KOSTER U. Oxidation of Zr-based metallic glasses in air [J]. *J Non-Cryst Solids*, 1999, 250/252: 719–723.
- [37] YAN M, SHEN J, SUN J F, ZOU J. Cooling rates effects on the microstructure of a Zr-based bulk metallic glass [J]. *Sci Tech Adv Mater*, 2006, 7: 806–811.
- [38] YAN M, SHEN J, SUN J F, ZOU J. Cooling rate-dependent as-cast microstructure and mechanical properties of Zr-based metallic glasses [J]. *J Mater Sci*, 2007, 42: 4233–4239.
- [39] LU K. Crystallization and its mechanism of amorphous alloys [D]. Shenyang: Institute of Metal Research, Chinese Academy of Science, 1990.
- [40] YAN M, SHEN J, ZOU J. A TEM study on the crystallization behavior of an yttrium doped Zr-based metallic glass [J]. *Intermetallics*, 2007, 15: 961–967.

(Edited by LI Xiang-qun)